Clinical Cancer Research

Phase I Study of the Novel Investigational NEDD8-Activating Enzyme Inhibitor Pevonedistat (MLN4924) in Patients with Relapsed/Refractory Multiple Myeloma or Lymphoma

Jatin J. Shah[1], Andrzej J. Jakubowiak[2], Owen A. O'Connor[3], Robert Z. Orlowski[1], R. Donald Harvey[4], Mitchell R. Smith[5], Daniel Lebovic[6], Catherine Diefenbach[7], Kevin Kelly[8], Zhaowei Hua[9], Allison J. Berger[9], George Mulligan[9], Hélène M. Faessel[9], Stephen Tirrell[9], Bruce J. Dezube[9], and Sagar Lonial[4]

Abstract

Purpose: Evaluate the safety, pharmacokinetic profile, pharmacodynamic effects, and antitumor activity of the first-in-class investigational NEDD8-activating enzyme (NAE) inhibitor pevonedistat (TAK-924/MLN4924) in patients with relapsed/refractory lymphoma or multiple myeloma.

Experimental Design: Patients with relapsed/refractory myeloma ($n = 17$) or lymphoma ($n = 27$) received intravenous pevonedistat 25 to 147 mg/m^2 on days 1, 2, 8, 9 (schedule A; $n = 27$) or 100 to 261 mg/m^2 on days 1, 4, 8, 11 (schedule B; $n = 17$) of 21-day cycles.

Results: Maximum tolerated doses were 110 mg/m^2 (schedule A) and 196 mg/m^2 (schedule B). Dose-limiting toxicities included febrile neutropenia, transaminase elevations, muscle cramps (schedule A), and thrombocytopenia (schedule B). Common adverse events included fatigue and nausea. Common grade $\geq$3 events were anemia (19%; schedule A), and neutropenia and pneumonia (12%; schedule B). Clinically significant myelosuppression was uncommon. There were no treatment-related deaths. Pevonedistat pharmacokinetics exhibited a biphasic disposition phase and approximate dose-proportional increases in systemic exposure. Consistent with the short mean elimination half-life of approximately 8.5 hours, little-to-no drug accumulation in plasma was seen after multiple dosing. Pharmacodynamic evidence of NAE inhibition included increased skin levels of CDT-1 and NRF-2 (substrates of NAE-dependent ubiquitin ligases), and increased NRF-2-regulated gene transcript levels in whole blood. Pevonedistat–NEDD8 adduct was detected in bone marrow aspirates, indicating pevonedistat target engagement in the bone marrow compartment. Three lymphoma patients had partial responses; 30 patients achieved stable disease.

Conclusions: Pevonedistat demonstrated anticipated pharmacodynamic effects in the clinical setting, a tolerable safety profile, and some preliminary evidence that may be suggestive of the potential for activity in relapsed/refractory lymphoma. *Clin Cancer Res; 22(1); 34–43. ©2015 AACR.*

Introduction

Regulated protein turnover via the ubiquitin–proteasome system (UPS) is central to the control of a wide variety of cellular processes (1). UPS dysregulation can lead to unrestrained cellular proliferation and/or failure to undergo programmed cell death, and development of cancer (2). Targeting the UPS was initially validated clinically with proteasome inhibitors, such as bortezomib and carfilzomib (3–5). Many proteins degraded by the UPS have important roles in cell signaling, cell-cycle progression, and apoptosis (6). These proteins are targeted for destruction when modified with a polyubiquitin chain by E3 ubiquitin ligases. The largest family is the Cullin–RING E3 ubiquitin ligases (CRLs), the activity of which is regulated by conjugation of ubiquitin-like protein NEDD8 (neural precursor cell expressed, developmentally downregulated 8) to the cullin proteins (7, 8). NEDD8-activating enzyme (NAE) controls NEDD8 conjugation and is required for CRL activity and proteasomal destruction of CRL substrates (7, 8).

[1]Lymphoma/Myeloma, The University of Texas MD Anderson Cancer Center, Houston, Texas. [2]Section of Hematology/Oncology, University of Chicago, Chicago, Illinois. [3]Center for Lymphoid Malignancies, Columbia University Medical Center, New York, New York. [4]Winship Cancer Institute, Emory University, Atlanta, Georgia. [5]Fox Chase Cancer Center, Philadelphia, Pennsylvania. [6]Hematology/Oncology, University of Michigan Comprehensive Cancer Center, Ann Arbor, Michigan. [7]New York University School of Medicine, NYU Perlmutter Cancer Center, New York, New York. [8]Department of Medicine, University of Southern California, Los Angeles, California. [9]Millennium Pharmaceuticals, Inc., Cambridge, MA, a wholly owned subsidiary of Takeda Pharmaceutical Company Ltd., Cambridge, Massachusetts.

Note: Supplementary data for this article are available at Clinical Cancer Research Online (http://clincancerres.aacrjournals.org/).

Corresponding Author: Jatin J. Shah, Lymphoma/Myeloma, The University of Texas MD Anderson Cancer Center, 1515 Holcombe Boulevard, Unit 0429, Houston, TX 77030. Phone: 713-792-2860; Fax: 713-794-5656; E-mail: jjshah@mdanderson.org

doi: 10.1158/1078-0432.CCR-15-1237

Translational Relevance

Targeting the ubiquitin–proteasome system (UPS), a key regulator of intracellular protein degradation, is an effective therapeutic approach in some hematologic cancers. Many proteins with roles in cell signaling and cell-cycle progression are targeted for UPS degradation by the Cullin–RING E3 ubiquitin ligases (CRLs), the activity of which is regulated by conjugation of ubiquitin-like protein NEDD8 to the cullin proteins. NEDD8-activating enzyme (NAE) controls NEDD8 conjugation and is therefore essential for CRL activity, making NAE inhibition a feasible therapeutic target. This study investigated pevonedistat (TAK-924/MLN4924), a novel investigational inhibitor of NAE, in patients with multiple myeloma or lymphoma, and demonstrated the validity of NAE inhibition as a therapeutic target and the anticipated pharmacodynamic effects in the clinical setting. The safety profile of single-agent pevonedistat in patients with multiple myeloma and lymphoma was generally tolerable, and there was preliminary evidence that may be suggestive of modest antitumor activity in relapsed/refractory lymphoma.

Pevonedistat is a first-in-class investigational small-molecule inhibitor of NAE (9, 10). NAE inhibition with pevonedistat prevents NEDD8 conjugation to CRLs via formation of pevonedistat–NEDD8 adduct (9), and leads to accumulation of CRL substrates in cell culture studies and human tumor xenografts (10). Pevonedistat is cytotoxic to tumor cell lines including solid tumors and hematologic malignancies, such as lymphoma, leukemia, and multiple myeloma (11–15), and has demonstrated antitumor activity in mouse xenograft models of several human malignancies (10–12, 15, 16), including acute myeloid leukemia (AML; ref. 12), diffuse large B-cell lymphoma (DLBCL; ref. 11), and multiple myeloma (15). Preclinical studies have investigated pevonedistat in combination with other agents. Pevonedistat plus bortezomib, dexamethasone, or doxorubicin demonstrated at least additive cytotoxic activity in multiple myeloma cell lines (13, 15), and pevonedistat significantly enhanced cytarabine (17) and azacitidine (18) cytotoxicity in AML cell lines.

In cell line studies, the primary phenotype observed following NAE inhibition with pevonedistat is a cell-cycle defect associated with inhibited CDT-1 (chromatin licensing and DNA replication factor-1) degradation and consequent DNA rereplication and DNA damage, leading to apoptosis (10, 11, 19, 20). Elevations of CDT-1 and NRF-2 [nuclear factor (erythroid derived 2)-related factor 2] protein levels (both CRL substrates) have been used as pharmacodynamic markers of NAE inhibition in preclinical models (10, 11). A second phenotype described in models of activated B-cell-like DLBCL involved NF-κB inhibition, resulting in apoptosis induction (11).

This phase I study was undertaken to evaluate the safety, pharmacokinetic profile, pharmacodynamic effects (including validation of pharmacodynamic markers of NAE inhibition in the clinical setting), and antitumor activity of pevonedistat in patients with relapsed and/or refractory lymphoma or multiple myeloma.

Patients and Methods

Patients

Patients were aged ≥18 years and had relapsed and/or refractory disease after ≥2 prior lines of therapy for multiple myeloma, any B- or T-cell non–Hodgkin lymphoma, Hodgkin lymphoma (HL), or Waldenström macroglobulinemia. Other eligibility criteria included Eastern Cooperative Oncology Group (ECOG) performance status of 0 to 2, life expectancy of >6 weeks, adequate bone marrow (absolute neutrophil count ≥1,000/mm^3, platelet count ≥75,000/mm^3), hepatic (bilirubin <upper limit of normal [ULN]; aspartate aminotransferase [AST], alanine aminotransferase [ALT], alkaline phosphatase ≤2.5 × ULN), renal (calculated creatinine clearance >50 mL/minute), and cardiac (B-type natriuretic peptide ≤1.5 × ULN; left ventricular ejection fraction ≥45% or pulmonary artery systolic pressure ≤1.5 × ULN) function, and evaluable disease.

Patients were excluded if they had received corticosteroids within 7 days, systemic antineoplastic therapy within 21 days, rituximab within 2 months (unless evidence of progressive disease since last rituximab dose), any investigational products within 28 days, or major surgery, radiotherapy, or systemic antibiotic therapy within 14 days prior to the first dose of study treatment. Other exclusion criteria included use of moderate or strong CYP3A inhibitors or inducers or a serious infection within 14 days prior to the first dose, a prothrombin time or activated partial thromboplastin time >1.5 × ULN, a history of a coagulopathy or bleeding disorder, or a requirement for warfarin which could not be switched to low molecular weight heparin. Patients with left ventricular ejection fraction <45% or pulmonary artery systolic pressure >1.5 × ULN as assessed by echocardiogram with Doppler; uncontrolled cardiovascular conditions, including cardiac arrhythmias, congestive heart failure, angina, or myocardial infarction within the past 6 months; or abnormalities on 12-lead ECG such as changes in rhythm and intervals considered by the investigator to be clinically significant were also excluded.

Review boards at all participating institutions approved the study, which was conducted according to International Conference on Harmonization Guidelines for Good Clinical Practice. All patients provided written informed consent prior to enrollment onto the study.

Study Design

This open-label, multicenter, phase I, dose-escalation study (ClinicalTrials.gov: NCT00722488) was conducted at eight sites in the United States between June 2008 and June 2012 for patients reported herein. The primary objectives were to determine the maximum tolerated dose (MTD) and safety profile of pevonedistat, describe pevonedistat pharmacokinetic and pharmacodynamic profiles in blood, and investigate pharmacodynamic effects in skin biopsies and bone marrow aspirates (patients with bone marrow involvement only). Secondary objectives included evaluation of disease response and pharmacokinetic–pharmacodynamic relationships.

Patients received escalating doses of pevonedistat by intravenous infusion over 1 hour on days 1, 2, 8, and 9 (schedule A) or days 1, 4, 8, and 11 (schedule B) of 21-day cycles. Schedule A was selected based on a dosing schedule that had been used in preclinical *in vivo* investigations (10, 11). Subsequently, based on observed toxicities and data from other studies, schedule B was selected, based on the standard dosing schedule for the

proteasome inhibitor bortezomib (21), to give a break between doses. The maximum permitted duration of the therapy was 12 months. In schedule A, dose escalation started at 25 mg/m^2, followed by 50 mg/m^2, 83 mg/m^2, and then doses 1.33 times the prior dose level. Schedule B dose escalation started at the schedule A MTD, with subsequent dose levels 1.33 times the prior dose level. A minimum of two patients were to be treated at each dose level before escalating. MTD determination was based on a Bayesian continual reassessment method. Once established during schedule A, the MTD level was expanded to approximately 14 patients (7 multiple myeloma and 7 lymphoma).

Patients who received all four scheduled doses, or had a dose-limiting toxicity (DLT) in cycle 1, were included in the DLT-evaluable population. DLT was defined as: grade $\geq$3 neutropenia with fever/infection, or grade 4 neutropenia for >7 days; a platelet count <10,000/mm^3, grade $\geq$3 thrombocytopenia with bleeding, or grade 4 thrombocytopenia for >7 days; grade $\geq$3 nonhematologic toxicity despite maximal supportive therapy, except arthralgia/myalgia, brief fatigue, or fever without neutropenia; grade $\geq$2 pevonedistat-related toxicities requiring dose reduction/discontinuation; or treatment delay >2 weeks due to lack of adequate recovery from toxicities.

Dose reduction was required for dose-limiting hematologic toxicity. For grade 3 nonhematologic toxicity, dosing was interrupted until resolution to grade $\leq$1, and then reinstated at the next lower dose level. Pevonedistat was discontinued for any grade 4 nonhematologic toxicity.

Assessments

Toxicities were recorded throughout the study until 30 days after last dose. Adverse events (AEs) were graded according to the National Cancer Institute's Common Terminology Criteria for AEs (NCI CTCAE) version 3.0.

For patients with lymphoma, CT of the chest, abdomen, and pelvis, and a PET scan from neck to mid-thighs were performed at screening and on day 21 of cycles 1, 3, and 5. From cycle 7, patients were evaluated using CT only every other cycle and at the end of study visit. Tumor response was assessed by the investigators using International Working Group criteria for patients with lymphoma (22).

For patients with multiple myeloma, a skeletal survey was performed at screening and radiographs were performed as needed to evaluate for disease progression if signs or symptoms of increased or new bone lesions were present. CT or MRI scans were performed as clinically indicated, at baseline, at the end of cycle 1, and every other cycle thereafter, to evaluate suspected extramedullary disease. Quantitative M-protein assessment and serum and urine immunofixation were performed at baseline, and at the end of cycle 1 and every alternate cycle thereafter. Disease status was assessed using the International Myeloma Working Group Uniform Response Criteria (23).

Pharmacokinetic and pharmacodynamic analyses

For pharmacokinetic analyses, serial blood samples were obtained during cycle 1 for determination of pevonedistat plasma concentrations. On schedule A, samples were obtained within 1 hour before infusion and immediately after completion of infusion on days 1, 2, 8, and 9. Additionally, samples were obtained: on day 1 at 30 minutes, 1, 2, 4, and 8 hours after completion of infusion; and on day 9 at 30 minutes, 1, 2, 4, 6, 9, 24, 72, and 144 hours after completion of infusion. On schedule B, samples were collected on days 1, 4, 8, and 11 within 1 hour (day 1) or within 10 minutes (days 4, 8, 11) before infusion as well as immediately after completion of infusion. Additionally, samples were obtained at 1, 2, 4, and 8 hours after completion of infusion and 24 and 48 hours after start of infusion on days 1 and 4. Bioanalytical assays were conducted at Tandem Labs. Plasma concentrations were measured using Good Laboratory Practice-validated liquid chromatography with tandem mass spectrometry. The dynamic range was 1 to 500 ng/mL for the low-range assay, and 75 to 7,500 ng/mL for the high-range assay. Noncompartmental methods (WinNonlin software, vs 6.2, Pharsight Corporation) were used to estimate pharmacokinetic parameters.

For pharmacodynamic analyses, whole blood was isolated in PAXgene tubes at screening, baseline, and during cycle 1: following pevonedistat administration on day 1 (at 4 and 8 hours), on day 2 predose, and on day 5 (schedule A); or following pevonedistat administration on days 1 and 11 (at 4, 8, and 23 hours), predose on days 4 and 11, and on day 15 (schedule B). RT-PCR was used to analyze expression in whole blood of eight genes shown to be induced by pevonedistat in preclinical studies (*ATF-3*, *GCLM*, *GSR*, *MAG1*, *NQO1*, *SLC7A11*, *SRXN1*, and *TXNRD1*; all except *MAG1* known to be regulated by NRF-2; ref. 24). Pharmacodynamic assays were performed at Asuragen (RT-PCR panel).

Raw data were transformed prior to the calculation of percentage change and assumptions were made for missing data. The percentage change from baseline in the relative expression of each of the eight genes of interest was calculated as $(2^{-(\text{post-baseline } \Delta Ct \,-\, \text{baseline } \Delta Ct)} - 1) \times 100$. The ΔCt was the mean *C*t (cycle threshold, a measure of mRNA gene expression, over the replicates) for each gene of interest, minus the mean *C*t for four housekeeping genes (18S, B2M, RPLP0, and UBC) calculated at each time point. A positive percentage change was equivalent to an increase in expression after dosing with pevonedistat. For *C*t values that were undetermined, the value 40 (the number of PCR cycles) was used for purposes of estimation of pharmacodynamic parameters and data summarization. Summary statistics were generated for the percentage change from baseline at each time point for each gene.

Skin punch biopsies (2 mm) for CDT-1 and NRF-2 IHC assays were performed at screening, and 3 to 6 hours after the cycle 1, day 2 (schedule A) or day 4 (schedule B) dose. The rationale for these investigations was to determine if biologically active levels of pevonedistat were achieved outside of the blood compartment.

IHC assays were performed at Millennium Pharmaceuticals, Inc. on five micrometer sections using the Ventana XT® autostainer. Antigen retrieval consisted of incubation with Ventana's CC1 antigen retrieval solution for 20 minutes and treatment with assay-specific antibodies. Antibodies to CDT-1 (Millennium Pharmaceuticals, Inc.) and NRF-2 (Epitomics Catalog #2178) were incubated for 1 hour at room temperature, labeled with Ventana's alkaline phosphatase ultra secondary antibodies for 32 minutes at room temperature, and developed with Ventana's NBT/BCIP substrate system. Slides were counterstained and imaged at 20$\times$ magnification using Aperio's whole-slide imaging scanner. Signal expression was calculated as the percentage stained area of the basal epithelial region, and quantified using Metamorph imaging software.

Bone marrow aspirates for pevonedistat–NEDD8 adduct and CD138 IHC assay were taken at screening and 2 to 6 hours after the cycle 1, day 2 (schedule A) or day 4 (schedule B) dose. Analyses

were performed at Millennium Pharmaceuticals, Inc. Aspirates were allowed to clot and then formalin-fixed and paraffin-embedded. An antibody specific for pevonedistat–NEDD8 adduct (Millennium Pharmaceuticals, Inc.) was incubated for 1 hour at 37ºC and labeled with Vector Laboratories goat anti-rabbit biotinylated secondary for 32 minutes at room temperature; Ventana's DAB Map system was used for detection of the biotinylated secondary. Similarly, a CD138 antibody (Ventana catalog #760-4248) was incubated for 1 hour at 37ºC and labeled with UltraMap™ HRP anti-mouse secondary antibody for 4 minutes at room temperature. Ventana's ChromoMap DAB Map system was used for detection of the HRP secondary. All slides were counterstained and imaged at 20× magnification using Aperio's whole-slide imaging scanner. CD138 staining was used to identify multiple myeloma cells, and presence of pevonedistat–NEDD8 adduct showed mechanism-based NAE inhibition in the bone marrow compartment.

Statistical methods

The MTD for each schedule was defined as the dose level closest to that predicted to result in a 25% DLT rate. MTD was predicted using a Bayesian continual reassessment method (25) algorithm based on observed toxicities in all the enrolled patients. The dose level at which the total number of enrolled patients reached six was to be considered the observed MTD. The dose–toxicity relationship was modeled by a single-parameter logistic model with a beta prior distribution. Cohorts of no more than two patients were dosed with pevonedistat at a given time. The decision to escalate, de-escalate, or expand the given dose was based on the model-estimated predicted MTD (PMTD). Patients were dosed at the dose level closest to the PMTD. Dose levels were predefined; skipping dose levels was not permitted. Descriptive statistics were used to summarize all data.

Results

Patient characteristics

Twenty-seven patients received pevonedistat on schedule A, and 17 patients received pevonedistat on schedule B. Patient demographics and baseline disease characteristics are summarized in Table 1. Patients were heavily pretreated (Supplementary Table SA1). All patients with multiple myeloma and two patients with lymphoma had been previously treated with bortezomib.

Table 1. Patient demographics and baseline characteristics in schedule A (days 1, 2, 8, and 9 of 21-day cycles) and schedule B (days 1, 4, 8, and 11 of 21-day cycles)

Characteristics	Schedule A *N* = 27	Schedule B *N* = 17
Median age, y (range)	62.0 (34–90)	58.0 (26–68)
Male, *n* (%)	17 (63)	13 (76)
Race, *n* (%)		
White	21 (78)	11 (65)
Black or African American	5 (19)	4 (24)
American Indian or Alaskan native	0	1 (6)
Not reported	1 (4)	1 (6)
ECOG performance status, *n* (%)		
0	11 (41)	3 (18)
1	13 (48)	13 (76)
2	2 (7)	1 (6)
3[a]	1 (4)	0
Patients with MM, *n* (%)	*n* = 15	*n* = 2
MM subtype, *n* (%)[b]		
IgG	10 (67)	2 (100)
IgA	4 (27)	1 (50)
Other	2 (13)	0
Median time since initial diagnosis, months (range)	78.0 (18–111)	81.5 (66–97)
Patients with lymphoma, *n* (%)	*n* = 12	*n* = 15
Lymphoma subtype, *n* (%)		
Follicular lymphoma	4 (33)	1 (7)
DLBCL	3 (25)	7 (47)
Small lymphocytic lymphoma/chronic lymphocytic leukemia	1 (8)	1 (7)
Mantle cell lymphoma	1 (8)	0
Lymphoplasmacytic lymphoma	1 (8)	0
Hodgkin lymphoma	1 (8)	4 (27)
PTCL	0	1 (7)
Splenic marginal zone B-cell lymphoma	0	1 (7)
Other	1 (8)	0
Bone marrow involvement, *n* (%)	5 (42)	3 (20)
Median time since primary diagnosis, months (range)	75.5 (19–197)	32.0 (1–102)

Abbreviations: PTCL, peripheral T-cell lymphoma, not otherwise specified.
[a]Protocol deviation.
[b]One patient in schedule A recorded as having MM subtypes of IgG and other: oligosecretory; 1 patient in schedule B recorded as having MM subtypes of IgG and IgA.

Dose escalation and MTD determination

Schedule A. Patients were treated at six pevonedistat dose levels: 25 ($n = 3$), 50 ($n = 2$), 65 ($n = 3$), 83 ($n = 2$), 110 ($n = 14$), and 147 ($n = 3$) mg/m^2. Twenty-two patients were DLT-evaluable; five were

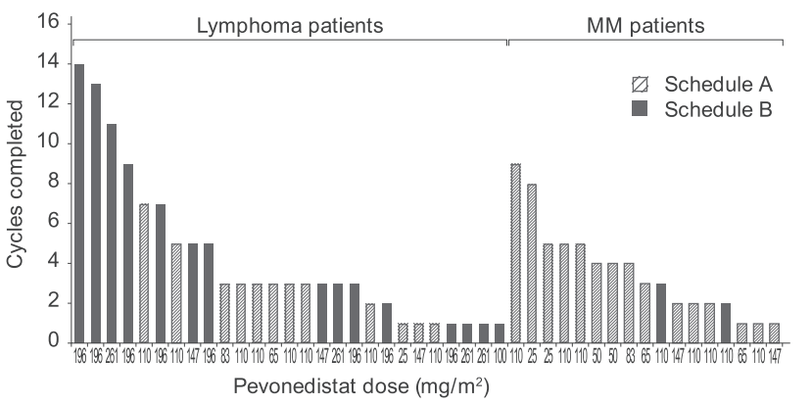

Figure 1.
Treatment duration with pevonedistat, by dose level and tumor type. Patients with MM and lymphoma received a median of 3 (range, 1–9) and 3 (range, 1–14) cycles, respectively. Fourteen patients (7 in each schedule) received ≥5 treatment cycles.

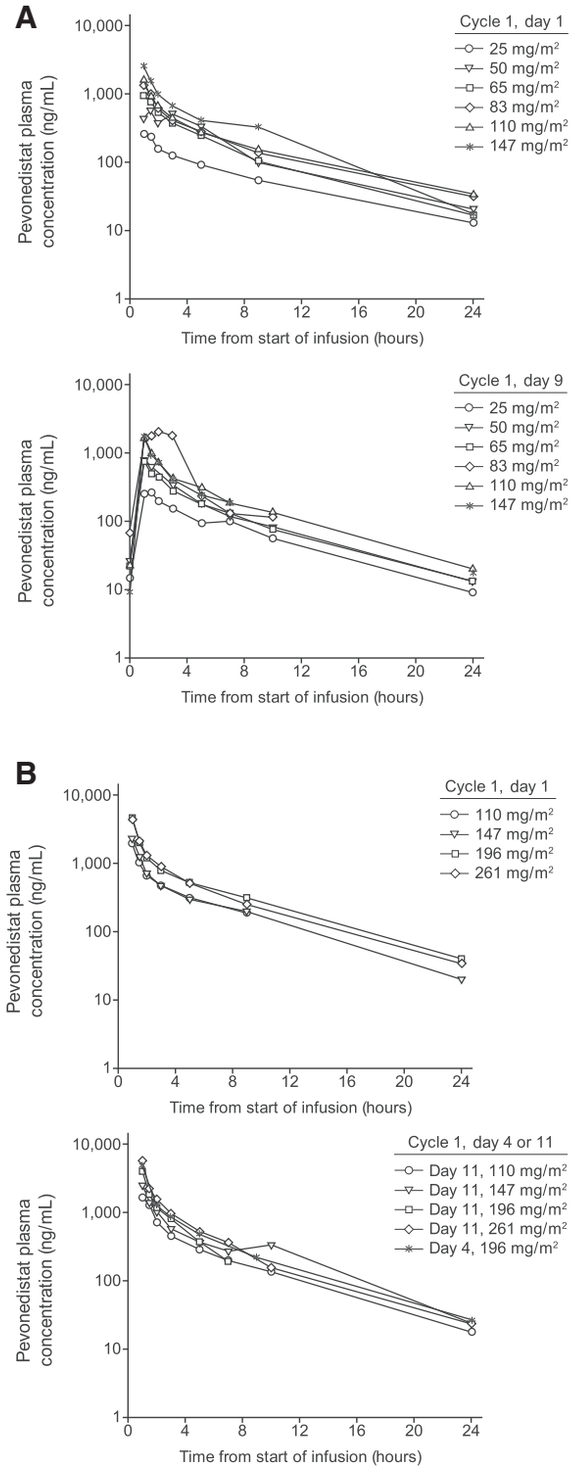

Figure 2.
Mean pevonedistat plasma concentration–time profiles on days 1 and 9 of schedule A (A) and days 1 and 4 (or, alternatively, day 11) of schedule B (B). Mean plasma concentration–time profiles of pevonedistat exhibited a biphasic disposition phase, characterized by an initial rapid decline at the end of the infusion, followed by a slower phase with plasma concentrations remaining quantifiable up to 24 hours (schedule A) or 48 hours (schedule B) after infusion at all doses.

excluded due to not receiving all four doses in cycle 1. Three patients experienced DLTs. One patient at 65 mg/m^2 had drug-related grade 4 febrile neutropenia on day 3, which resolved by day 10 following dose reduction to 50 mg/m^2. One patient at 110 mg/m^2 had drug-related grade 3 AST/ALT elevation on day 2, which resolved by day 8 following dose reduction to 83 mg/m^2. One patient at 147 mg/m^2 had grade 3 muscle cramps on day 2, which resolved within 48 hours following pevonedistat discontinuation. Due to the severity of this AE, it was decided to no longer dose patients above 110 mg/m^2 in schedule A. Three additional patients were enrolled to the 110 mg/m^2 cohort, and with six patients treated at this dose level the MTD was determined to be 110 mg/m^2.

Schedule B. Patients were treated at five pevonedistat dose levels: 110 ($n = 2$), 147 ($n = 2$), 196 ($n = 8$), 261 ($n = 4$); one patient received 100 mg/m^2 after this dose level was identified for further evaluation based on safety evaluation across all pevonedistat trials. Thirteen patients were DLT-evaluable. One patient at 110 mg/m^2 experienced grade 3 thrombocytopenia on day 15; the patient discontinued after cycle 2, day 1 due to disease progression, and thrombocytopenia was ongoing at the end-of-study visit 12 days later. Following the occurrence of acute severe toxicities at high pevonedistat doses in a few patients in another study (NCT01011530), it was decided not to administer pevonedistat at doses >200 mg/m^2. Therefore, although no DLTs were observed at 261 mg/m^2, 196 mg/m^2 was selected as the schedule B MTD. Unlike in schedule A, this cohort was not expanded to 14 patients per the sponsor's decision, following a cross-program review, to move forward with studies of pevonedistat in combination with standard-of-care therapies.

Treatment exposure and safety

Patients received a median of three cycles of treatment on both schedules (schedule A, range, 1–9; schedule B, range, 1–14; Fig. 1). All patients have discontinued pevonedistat due to progressive disease/symptomatic deterioration (schedule A, $n = 19$; schedule B, $n = 15$), consent withdrawal ($n = 5$; $n = 1$), occurrence of an AE ($n = 2$; $n = 1$), or unsatisfactory therapeutic response ($n = 1$, $n = 0$).

AEs reported in ≥15% of patients and grade ≥3 AEs reported in >1 patient on either schedule are shown in Table 2. Transaminase elevations were clinically asymptomatic and reversible with dose modification. Myelosuppression was limited, with anemia the only hematologic toxicity reported in >20% of patients overall. There was no requirement for growth factor or transfusion support. Peripheral neuropathy was limited (11%) and similar between schedules (Table 2). No grade 4 AEs were reported at the MTD in either schedule.

Eight patients each on schedule A (30%) and schedule B (47%) experienced serious AEs (SAEs). On schedule A, four patients had SAEs considered related to pevonedistat: grade 4 anemia and grade 3 generalized body pain; grade 4 febrile neutropenia (DLT); grade 2 pyrexia; and grade 2 orthostatic hypotension. On schedule B, two patients had drug-related SAEs: grade 4 neutropenia and grade 3 bacteremia; and grade 2 pyrexia and grade 2 sinus tachycardia. Two patients in schedule A died on study due to progressive disease; there were no treatment-related deaths.

Pharmacokinetic profile

Mean plasma concentration–time profiles of pevonedistat exhibited a biphasic disposition phase (Fig. 2). In general,

Table 2. The most common AEs of any grade reported in ≥15% of patients in either schedule and of grade ≥3 reported in >1 patient on either schedule

	Schedule A ($n = 27$)		Schedule B ($n = 17$)	
AE, *n* (%)	**All grades**	**Grade ≥3**	**All grades**	**Grade ≥3**
Any AE	27 (100)	16 (59)	17 (100)	12 (71)
Hematologic AEs				
Anemia	7 (26)	5 (19)	3 (18)	1 (6)
Thrombocytopenia	3 (11)	1 (4)	3 (18)	1 (6)[a]
Neutropenia	2 (7)	2 (7)	2 (12)	2 (12)
Nonhematologic AEs				
Fatigue	18 (67)	2 (7)	12 (71)	1 (6)
ALT increased	12 (44)	1 (4)[a]	4 (24)	1 (6)
AST increased	12 (44)	2 (7)[a]	2 (12)	0
Nausea	12 (44)	0	13 (76)	0
Pyrexia	11 (41)	0	8 (47)	1 (6)
Constipation	10 (37)	0	5 (29)	0
Myalgia	10 (37)	0	10 (59)	0
Diarrhea	7 (26)	1 (4)	8 (47)	0
Headache	7 (26)	0	9 (53)	0
Vomiting	7 (26)	0	10 (59)	0
Blood alkaline phosphatase increased	6 (22)	0	1 (6)	0
Decreased appetite	6 (22)	0	10 (59)	0
Dizziness	6 (22)	0	8 (47)	0
Hypomagnesemia	6 (22)	0	1 (6)	0
Pain	6 (22)	1 (4)	5 (29)	1 (6)
Chills	5 (19)	0	6 (35)	0
Dyspnea	5 (19)	1 (4)	4 (24)	1 (6)
Hypercalcemia	5 (19)	2 (7)	1 (6)	0
Hypophosphatemia	5 (19)	3 (11)	1 (6)	1 (6)
Vision blurred	5 (19)	0	0	0
Blood creatinine increased	4 (15)	0	0	0
Hyperkalemia	4 (15)	1 (4)	0	0
Muscle spasms	4 (15)	1 (4)[a]	10 (59)	1 (6)
Pain in extremity	4 (15)	0	5 (29)	0
Back pain	3 (11)	0	4 (24)	0
Insomnia	3 (11)	0	4 (24)	0
Peripheral edema	3 (11)	0	3 (18)	0
Upper respiratory tract infection	3 (11)	0	3 (18)	1 (6)
Peripheral neuropathies NEC[b]	3 (11)	0	2 (12)	0
Asthenia	2 (7)	0	3 (18)	0
Cough	2 (7)	0	5 (29)	0
Dehydration	2 (7)	0	3 (18)	1 (6)
Paresthesia	2 (7)	0	5 (29)	0
Productive cough	2 (7)	0	3 (18)	0
Sinus tachycardia	2 (7)	1 (4)	3 (18)	0
Abdominal discomfort	1 (4)	0	3 (18)	0
Hyperbilirubinemia	1 (4)	0	5 (29)	1 (6)
Pneumonia	1 (4)	1 (4)	3 (18)	2 (12)
Weight decreased	1 (4)	0	3 (18)	0
Dyspepsia	0	0	3 (18)	0
Dyspnea exertional	0	0	3 (18)	0

Abbreviation: NEC, not elsewhere classified.

[a]One DLT.

[b]High-level term, incorporating 3 "neuropathy peripheral" (2 schedule A, 1 schedule B), 1 peripheral sensory neuropathy (schedule A), and 1 peripheral sensorimotor neuropathy (schedule B); 3 multiple myeloma patients with prior bortezomib had peripheral neuropathy, plus 2 lymphoma patients without prior bortezomib.

acknowledging the relatively small cohort sizes, approximate dose-proportional increases in mean C_{max} and $AUC_{0-24\ h}$ were seen across the 25 to 147 mg/m^2 dose levels in schedule A (Supplementary Table SA2) and the 100 to 261 mg/m^2 dose levels in schedule B (Supplementary Table SA3).

Pharmacokinetic parameters from 13 and 7 patients receiving the MTDs on schedules A and B, respectively, are summarized in Table 3. Terminal disposition phase was adequately characterized in five patients at the schedule B MTD; mean plasma elimination half-life was estimated to be 8.5 hours (range, 7.7–9.1). Consistent with this, pevonedistat systemic exposures were similar between days 1 and 9 on schedule A and days 1 and 4 (or, alternatively, day 11) on schedule B, indicating little or no drug accumulation in plasma.

Pharmacodynamic effects

Pevonedistat induced the expected pharmacodynamic effects in whole blood, indicating NAE inhibition; expression of NRF-2-regulated genes (and MAG-1) was increased following pevonedistat administration on cycle 1, day 1 versus baseline across the 25 to 261 mg/m^2 dose range (data at MTDs shown in Supplementary Table SA4), notably *NQO1*, for which maximal changes from baseline ranged from approximately 250% to 400% and 700% to 800% at doses of 25 to 83 mg/m^2 and 110

Table 3. Pharmacokinetic parameters of pevonedistat during cycle 1 in patients receiving pevonedistat at the MTD determined in each schedule

	Schedule A, 110 mg/m^2		Schedule B, 196 mg/m^2	
Parameter	**Day 1, $n = 13$**	**Day 9, $n = 9$**	**Day 1, $n = 7$**	**Day 4, $n = 6$**
C_{max}, ng/mL	1,502 (33)	1,683 (28)	4,565 (24)	3,751 (53)
T_{max}, hour	1.02 (1.0–1.3)	1.08 (1.0–1.1)	1.1 (1.0–1.1)	1.02 (0.9–1.1)
$AUC_{0\text{-}24\ h}$, ng·hour/mL	4,685 (23)	4,833 (19)[a]	10,830 (19)[b]	8,309 (39)
$AUC_{0\text{-}\tau}$, ng·hour/mL	4,685 (23)	4,833 (19)[a]	12,367 (13)[c]	NE
$t_{1/2}$, hour	NE	NE	8.5 (0.6)[d]	NE
CL_p, L/hour	NE	NE	28.3 (3)[e]	NE
V_{ss}, L	NE	NE	158 (9)[e]	NE

NOTES: Parameters are reported as geometric mean (% coefficient of variation), except for T_{max}, which is reported as median (range), and $t_{1/2}$, which is reported as the arithmetic mean (standard deviation).

Abbreviations: NE, not estimated. Due to limited time points in the terminal disposition phase, an estimate of pevonedistat elimination half-life could not be obtained for schedule A. C_{max}, maximum observed concentration; T_{max}, time to reach C_{max}; $AUC_{0\text{-}24h}/AUC_{0\text{-}\tau}$, area under the concentration–time curve from time zero to 24 hours/to the end of dosing interval, where the dosing interval, τ, is equal to 24 and 72 hours for schedules A and B, respectively; $t_{1/2}$, terminal disposition half-life; CL_p, plasma clearance; V_{ss}, steady-state volume of distribution.

[a]$n = 7$.

[b]$n = 6$.

[c]$n = 4$.

[d]$n = 5$.

[e]$n = 3$.

to 261 mg/m^2, respectively (data not shown). These effects generally appeared to increase with increasing systemic exposure to pevonedistat.

IHC assessment of skin biopsies showed increases in CDT-1 and NRF-2 expression levels following the second dose of pevonedistat in cycle 1, compared with baseline, indicating NAE pathway inhibition by pevonedistat in the peripheral tissue. Figure 3 shows fold-change in CDT-1 expression versus baseline among evaluable patients, and representative IHC images of CDT-1 and NRF-2 staining. For NRF-2, 19 patients treated on schedule A at pevonedistat 25 to 147 mg/m^2 showed a mean 185-fold [SD 356; median 39.4-fold (range, 0–1,483)] increase; 3 additional patients on schedule A had NRF-2 increases post-dose from a baseline value of zero (data not shown). No correlation could be found with individual CDT-1 or NRF-2 changes and pevonedistat systemic exposures.

IHC assays of bone marrow aspirates from patients with multiple myeloma or lymphoma with bone marrow involvement demonstrated the presence of pevonedistat–NEDD8 adduct in post-dose samples from 11 of 13 evaluable patients on schedules A and B. In one patient treated at 25 mg/m^2, pevonedistat–NEDD8 adduct was not detected in either the predose or post-dose sample, and one pair of samples showed adduct in the predose but not the post-dose sample, indicating a likely sample switch. A representative image is shown in Supplementary Fig. SA1, indicating pevonedistat target engagement in the bone marrow compartment.

Antitumor activity

One patient in schedule A and two in schedule B achieved partial responses (PRs). A 34-year-old male with relapsed nodular sclerosis HL achieved a PR with pevonedistat 110 mg/m^2 (schedule A) after five cycles, and had progressive disease on cycle 7, day 21. A 47-year-old male with relapsed DLBCL achieved a PR after three cycles of pevonedistat 196 mg/m^2 (schedule B) and remained on study to cycle 9, day 18, when he experienced disease progression. A 65-year-old female with relapsed peripheral T-cell lymphoma achieved a PR with pevonedistat 196 mg/m^2 (schedule B) in cycle 1 (day 21) that lasted two cycles until disease progression. Further patient details are provided in Supplementary Table SA5.

An additional 30 of 42 (71%) response-evaluable patients (treated patients who had $\geq$1 post-baseline disease assessment; $n = 19$, schedule A, $n = 11$, schedule B; $n = 17$ lymphoma, $n = 13$ multiple myeloma) achieved stable disease (SD), 12 of whom ($n = 6$ in each schedule) received $\geq$5 cycles. Of these 12, 7 patients with lymphoma had SD lasting 3.25 to 9.53 months and 5 patients with multiple myeloma had stable disease lasting 3.22 to 6.01 months (Supplementary Table SA6).

Discussion

Targeting the UPS is an effective therapeutic approach in human cancers, as demonstrated by the clinical development of proteasome inhibitors (3–5). Other therapeutic targets within the UPS are being investigated with the aim of affecting specific substrate proteins and signaling pathways of importance in human cancers (26, 27), without disrupting degradation of all UPS-processed proteins, as occurs with 26S proteasome inhibition (28). Inhibition of the NEDD8 conjugation pathway has emerged as a feasible therapeutic target (29).

This is the first reported study of pevonedistat in multiple myeloma and lymphoma. Pevonedistat had a generally manageable safety profile over a median treatment duration of three cycles. Approximately two thirds of patients experienced grade $\geq$3 AEs, with only anemia and hypophosphatemia on schedule A and neutropenia and pneumonia on schedule B reported in >10% of patients. The commonly reported elevations in liver enzymes were generally clinically asymptomatic and resolved to baseline. Furthermore, limited myelosuppression may make pevonedistat a suitable agent for use in combination with cytotoxic chemotherapy, or a feasible therapy for patients unable or unwilling to receive standard supportive measures for hematologic toxicity. Notably, the peripheral neuropathy rate was limited, at 11%.

The pevonedistat MTD was 110 mg/m^2 on schedule A and 196 mg/m^2 on schedule B. DLTs were observed relatively infrequently; in schedule A three DLTs of febrile neutropenia, transaminase elevations, and muscle cramps were observed, and in schedule B a single DLT of thrombocytopenia was observed. During schedule A, the severity of grade 3 muscle cramps prompted a decision to no

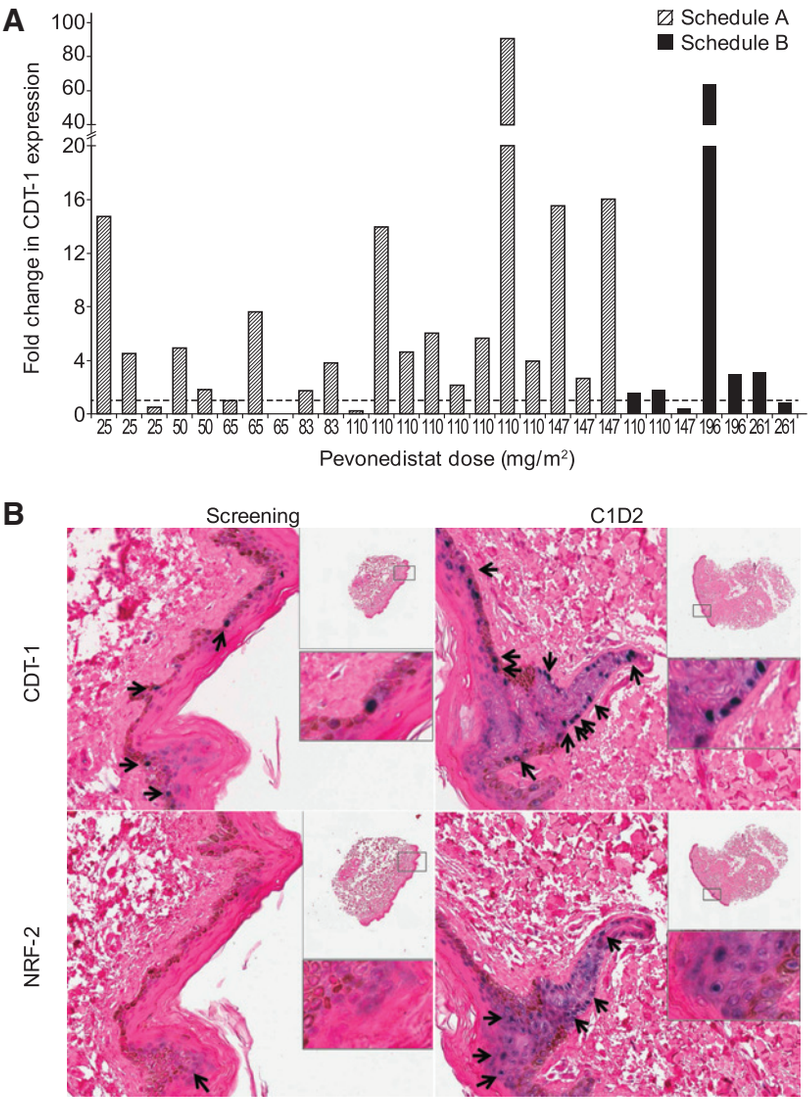

Figure 3.
Pevonedistat treatment increased CDT-1 and NRF-2 levels compared with baseline. A, fold-change from baseline in CDT-1 expression in skin biopsies obtained 3 to 6 hours after the second dose of pevonedistat in cycle 1 (day 2 on schedule A, day 4 on schedule B). B, representative IHC images of skin biopsy sections stained for CDT-1 and NRF-2 taken at baseline and on cycle 1, day 2 from a patient enrolled in the 83-mg/m^2 dose level on schedule A. Arrows and blue/purple staining indicate CDT-1 or NRF-2–positive staining.

longer dose patients above 110 mg/m^2, and in schedule B, although no DLTs were observed at 261 mg/m^2, toxicities observed in another study of pevonedistat (NCT01011530) prompted a program-wide safety review and a subsequent decision not to continue dosing at this higher end of the dosing range was enacted across clinical trials. Additionally, as noted in the Results, a cross-program review resulted in the decision to move forward with studies of pevonedistat in combination with standard-of-care therapies, and thus schedule B was not expanded at the MTD. Of note, the MTD in a separate phase 1 study of pevonedistat in patients with AML and myelodysplastic syndromes (MDS), using the same dosing as schedule B (days 1, 4, 8, and 11), was determined to be 83 mg/m^2 (30). This MTD may have been lower due to the population of relapsed/refractory AML/MDS patients being sicker than the patients with lymphoma/multiple myeloma in the present study or due to inherent differences between the diseases.

Pharmacokinetic analyses revealed a general increase in pevonedistat systemic exposure with increasing dose, and a half-life of 8.5 hours; consistent with this, little or no drug accumulation was seen following multiple dosing on either schedule. Analyses of whole blood, skin biopsies, and bone marrow aspirates demonstrated that pevonedistat exerted predicted pharmacodynamic effects, including increased levels of CDT-1 and NRF-2, and pevonedistat–NEDD8 adduct formation. Our findings represent important validation in the clinic of the pharmacodynamic markers of NAE inhibition and target engagement demonstrated in preclinical investigations (9–11).

Our study provides some preliminary evidence that may be suggestive of modest antitumor activity of single-agent pevonedistat in heavily pretreated patients in both dosing schedules, with three lymphoma patients achieving a PR. A further 71% of patients achieved SD, with 12 patients receiving $\geq$5 cycles. PRs were seen only in patients with lymphoma, with best responses of only SD seen in patients with multiple myeloma. Of potential importance, all patients with multiple myeloma and two patients with lymphoma had received prior bortezomib. Higher levels of proteasome maturation protein (POMP) have been seen in

bortezomib-resistant cell lines, and overexpression of NRF-2 has been shown to induce POMP and increase proteasome chymotrypsin activity (31); thus, increased NRF-2 levels following NAE inhibition, together with prior proteasome inhibition, may be associated with compensatory increases in POMP and possibly resistance to further UPS inhibition. Furthermore, lack of response in patients with multiple myeloma with pevonedistat may possibly be associated with limited induction of the endoplasmic reticulum (ER) stress response (32), compared with proteasome inhibition with bortezomib or ixazomib, for which ER stress has been linked with antimyeloma activity preclinically (33–35) and clinically (36).

In conclusion, this phase I study of pevonedistat demonstrated the validity of NAE inhibition as a therapeutic target and the anticipated pharmacodynamic effects in the clinical setting. We also report the safety profile of pevonedistat in patients with multiple myeloma and lymphoma and some preliminary evidence that is suggestive of the potential for modest activity in patients with relapsed/refractory lymphoma. Further to this single-agent activity, plus some modest clinical activity in patients with relapsed and/or refractory AML and MDS (30), rational combination strategies have been investigated, including pevonedistat plus azacitidine in patients with AML considered unfit for intensive induction therapy (NCT01814826; ref. 37); future clinical testing is expected to include lymphoma, AML, and MDS, although additional testing in multiple myeloma may not be warranted without additional research to support enrollment of a specific patient population. In patients with advanced solid tumors, rational combination strategies are being investigated, including pevonedistat plus docetaxel, gemcitabine, or carboplatin-paclitaxel (NCT01862328).

Disclosure of Potential Conflicts of Interest

O.A. O'Connor is a consultant/advisory board member for Millennium Pharmaceuticals, Inc. R.Z. Orlowski is a consultant/advisory board member for Millennium Pharmaceuticals, Inc., and reports receiving commercial research grants from Millennium Pharmaceuticals, Inc., D. Lebovic reports receiving speakers bureau honoraria from and is a consultant/advisory board member for Millennium Pharmaceuticals, Inc. S. Lonial is a consultant/advisory board member for Bristol-Myers Squibb, Celgene, Janssen, Millennium Pharmaceuticals, Inc., Novartis, and Onyx. No potential conflicts of interest were disclosed by the other authors.

Authors' Contributions

Conception and design: J.J. Shah, R.Z. Orlowski, M.R. Smith, A.J. Berger, G. Mulligan, H. Faessel, B.J. Dezube, S. Lonial

Development of methodology: A.J. Berger, G. Mulligan, B.J. Dezube

Acquisition of data (provided animals, acquired and managed patients, provided facilities, etc.): J.J. Shah, A.J. Jakubowiak, O.A. O'Connor, R.Z. Orlowski, R.D. Harvey, M.R. Smith, D. Lebovic, C. Diefenbach, K. Kelly, G. Mulligan, H. Faessel, B.J. Dezube, S. Lonial

Analysis and interpretation of data (e.g., statistical analysis, biostatistics, computational analysis): J.J. Shah, O.A. O'Connor, R.Z. Orlowski, R.D. Harvey, K. Kelly, Z. Hua, A.J. Berger, G. Mulligan, H. Faessel, B.J. Dezube, S. Lonial

Writing, review, and/or revision of the manuscript: J.J. Shah, A.J. Jakubowiak, O.A. O'Connor, R.Z. Orlowski, R.D. Harvey, M.R. Smith, D. Lebovic, C. Diefenbach, K. Kelly, Z. Hua, A.J. Berger, G. Mulligan, H. Faessel, B.J. Dezube, S. Lonial

Administrative, technical, or material support (i.e., reporting or organizing data, constructing databases): J.J. Shah, S. Tirrell, B.J. Dezube

Study supervision: J.J. Shah, B.J. Dezube

Acknowledgments

The authors thank Dr Stephen J. Blakemore, a former employee of Millennium Pharmaceuticals, Inc., a wholly owned subsidiary of Takeda Pharmaceutical Company Ltd., for helpful discussions and critical review during the development of the manuscript. The authors also thank Steve Hill of FireKite, an Ashfield company, part of UDG Healthcare plc, for writing support during the development of this article, which was funded by Millennium Pharmaceuticals, Inc.

Grant Support

This study was funded by Millennium Pharmaceuticals, Inc., a wholly owned subsidiary of Takeda Pharmaceutical Company Ltd.

The costs of publication of this article were defrayed in part by the payment of page charges. This article must therefore be hereby marked *advertisement* in accordance with 18 U.S.C. Section 1734 solely to indicate this fact.

Received May 29, 2015; revised August 10, 2015; accepted August 11, 2015; published OnlineFirst November 11, 2015.

References

1. Hershko A. The ubiquitin system for protein degradation and some of its roles in the control of the cell division cycle. Cell Death Differ 2005; 12:1191–7.
2. Ciechanover A. Intracellular protein degradation: from a vague idea thru the lysosome and the ubiquitin-proteasome system and onto human diseases and drug targeting. Cell Death Differ 2005;12:1178–90.
3. McBride A, Ryan PY. Proteasome inhibitors in the treatment of multiple myeloma. Expert Rev Anticancer Ther 2013;13:339–58.
4. O'Connor OA, Wright J, Moskowitz C, Muzzy J, Gregor-Cortelli B, Stubblefield M, et al. Phase II clinical experience with the novel proteasome inhibitor bortezomib in patients with indolent non-Hodgkin's lymphoma and mantle cell lymphoma. J Clin Oncol 2005;23:676–84.
5. O'Connor OA, Portlock C, Moskowitz C, Hamlin P, Straus D, Gerecitano J, et al. Time to treatment response in patients with follicular lymphoma treated with bortezomib is longer compared with other histologic subtypes. Clin Cancer Res 2010;16:719–26.
6. Herrmann J, Lerman LO, Lerman A. Ubiquitin and ubiquitin-like proteins in protein regulation. Circ Res 2007;100:1276–91.
7. Podust VN, Brownell JE, Gladysheva TB, Luo RS, Wang C, Coggins MB, et al. A Nedd8 conjugation pathway is essential for proteolytic targeting of p27Kip1 by ubiquitination. Proc Natl Acad Sci U S A 2000; 97:4579–84.
8. Read MA, Brownell JE, Gladysheva TB, Hottelet M, Parent LA, Coggins MB, et al. Nedd8 modification of cul-1 activates SCF(beta(TrCP))-dependent ubiquitination of IkappaBalpha. Mol Cell Biol 2000;20: 2326–33.
9. Brownell JE, Sintchak MD, Gavin JM, Liao H, Bruzzese FJ, Bump NJ, et al. Substrate-assisted inhibition of ubiquitin-like protein-activating enzymes: the NEDD8 E1 inhibitor MLN4924 forms a NEDD8-AMP mimetic in situ. Mol Cell 2010;37:102–11.
10. Soucy TA, Smith PG, Milhollen MA, Berger AJ, Gavin JM, Adhikari S, et al. An inhibitor of NEDD8-activating enzyme as a new approach to treat cancer. Nature 2009;458:732–6.
11. Milhollen MA, Traore T, Duffy J, Thomas MP, Berger AJ, Dang L, et al. MLN4924, a NEDD8-activating enzyme inhibitor, is active in diffuse large B-cell lymphoma models: rationale for treatment of NF-{kappa}B-dependent lymphoma. Blood 2010;116:1515–23.
12. Swords RT, Kelly KR, Smith PG, Garnsey JJ, Mahalingam D, Medina E, et al. Inhibition of NEDD8-activating enzyme: a novel approach for the treatment of acute myeloid leukemia. Blood 2010;115:3796–800.

13. Gu Y, Kaufman JL, Bernal L, Torre C, Matulis SM, Harvey RD, et al. MLN4924, an NAE inhibitor, suppresses AKT and mTOR signaling via upregulation of REDD1 in human myeloma cells. Blood 2014;123:3269–76.
14. Godbersen JC, Humphries LA, Danilova OV, Kebbekus PE, Brown JR, Eastman A, et al. The Nedd8-activating enzyme inhibitor MLN4924 thwarts microenvironment-driven NF-kappaB activation and induces apoptosis in chronic lymphocytic leukemia B cells. Clin Cancer Res 2014;20: 1576–89.
15. McMillin DW, Jacobs HM, Delmore JE, Buon L, Hunter ZR, Monrose V, et al. Molecular and cellular effects of NEDD8-activating enzyme inhibition in myeloma. Mol Cancer Ther 2012;11:942–51.
16. Luo Z, Yu G, Lee HW, Li L, Wang L, Yang D, et al. The Nedd8-activating enzyme inhibitor MLN4924 induces autophagy and apoptosis to suppress liver cancer cell growth. Cancer Res 2012;72:3360–71.
17. Nawrocki ST, Kelly KR, Smith PG, Keaton M, Carraway H, Sekeres MA, et al. The NEDD8-activating enzyme inhibitor MLN4924 disrupts nucleotide metabolism and augments the efficacy of cytarabine. Clin Cancer Res 2015;21:439–47.
18. Smith PG, Traore T, Grossman S, Narayanan U, Carew JS, Lublinsky AR, et al. Azacitidine/decitabine synergism with the NEDD8-activating enzyme inhibitor MLN4924 in pre-clinical AML models [abstract]. Blood 2011;118:578.
19. Milhollen MA, Narayanan U, Soucy TA, Veiby PO, Smith PG, Amidon B. Inhibition of NEDD8-activating enzyme induces rereplication and apoptosis in human tumor cells consistent with deregulating CDT1 turnover. Cancer Res 2011;71:3042–51.
20. Lin JJ, Milhollen MA, Smith PG, Narayanan U, Dutta A. NEDD8-targeting drug MLN4924 elicits DNA rereplication by stabilizing Cdt1 in S phase, triggering checkpoint activation, apoptosis, and senescence in cancer cells. Cancer Res 2010;70:10310–20.
21. Richardson PG, Sonneveld P, Schuster MW, Irwin D, Stadtmauer EA, Facon T, et al. Bortezomib or high-dose dexamethasone for relapsed multiple myeloma. N Engl J Med 2005;352:2487–98.
22. Cheson BD, Pfistner B, Juweid ME, Gascoyne RD, Specht L, Horning SJ, et al. Revised response criteria for malignant lymphoma. J Clin Oncol 2007;25:579–86.
23. Durie BG, Harousseau JL, Miguel JS, Blade J, Barlogie B, Anderson K, et al. International uniform response criteria for multiple myeloma. Leukemia 2006;20:1467–73.
24. Chorley BN, Campbell MR, Wang X, Karaca M, Sambandan D, Bangura F, et al. Identification of novel NRF2-regulated genes by ChIP-Seq: influence on retinoid X receptor alpha. Nucleic Acids Res 2012;40:7416–29.
25. O'Quigley J, Pepe M, Fisher L. Continual reassessment method: a practical design for phase 1 clinical trials in cancer. Biometrics 1990;46:33–48.
26. Micel LN, Tentler JJ, Smith PG, Eckhardt GS. Role of ubiquitin ligases and the proteasome in oncogenesis: novel targets for anticancer therapies. J Clin Oncol 2013;31:1231–8.
27. Pal A, Young MA, Donato NJ. Emerging potential of therapeutic targeting of ubiquitin-specific proteases in the treatment of cancer. Cancer Res 2014;74:4955–66.
28. Esseltine DL, Mulligan G. An historic perspective of proteasome inhibition. Semin Hematol 2012;49:196–206.
29. Soucy TA, Dick LR, Smith PG, Milhollen MA, Brownell JE. The NEDD8 conjugation pathway and its relevance in cancer biology and therapy. Genes Cancer 2010;1:708–16.
30. Swords RT, Erba HP, DeAngelo DJ, Bixby DL, Altman JK, Maris M, et al. Pevonedistat (MLN4924), a First-in-Class NEDD8-activating enzyme inhibitor, in patients with acute myeloid leukaemia and myelodysplastic syndromes: a phase 1 study. Br J Haematol 2015;169: 534–43.
31. Li B, Wang H, Orlowski RZ. Proteasome maturation protein (pomp) is associated with proteasome inhibitor resistance in myeloma, and its suppression enhances the activity of bortezomib and carfilzomib [abstract]. Blood 2013;122:280.
32. Liao H, Liu XJ, Blank JL, Bouck DC, Bernard H, Garcia K, et al. Quantitative proteomic analysis of cellular protein modulation upon inhibition of the NEDD8-activating enzyme by MLN4924. Mol Cell Proteomics 2011;10: M111.
33. Chauhan D, Tian Z, Zhou B, Kuhn D, Orlowski R, Raje N, et al. In vitro and in vivo selective antitumor activity of a novel orally bioavailable proteasome inhibitor MLN9708 against multiple myeloma cells. Clin Cancer Res 2011;17:5311–21.
34. Kraus M, Malenke E, Gogel J, Muller H, Ruckrich T, Overkleeft H, et al. Ritonavir induces endoplasmic reticulum stress and sensitizes sarcoma cells toward bortezomib-induced apoptosis. Mol Cancer Ther 2008;7: 1940–8.
35. Obeng EA, Carlson LM, Gutman DM, Harrington WJ Jr, Lee KP, Boise LH. Proteasome inhibitors induce a terminal unfolded protein response in multiple myeloma cells. Blood 2006;107:4907–16.
36. Leung-Hagesteijn C, Erdmann N, Cheung G, Keats JJ, Stewart AK, Reece DE, et al. Xbp1s-negative tumor B cells and pre-plasmablasts mediate therapeutic proteasome inhibitor resistance in multiple myeloma. Cancer Cell 2013;24:289–304.
37. Swords RT, Savona MR, Maris MB, Erba HP, Hua Z, Faessel H, et al. First-in-class NAE inhibitor MLN4924 in combination with azacitidine for acute myeloid leukemia (AML) patients considered unfit for conventional chemotherapy: results from the C15009 trial [abstract]. Haematologica 2014;99:223–4, (S650).